Axial strain dependence of all-fiber acousto-optic tunable filters

Kwang Jo Lee,[1,4] In-Kag Hwang,[1,*] Hyun Chul Park,[2] and Byoung Yoon Kim[3]

[1]*Department of Physics, Chonnam National University, 300 Yongbong-dong, Buk-gu, Gwangju, 500-757, Korea*
[2]*Instrumentation & Control Research Group, POSLAB, 1, Goedong-dong, Nam-gu, Pohang, Gyeongbuk, 790-300, Korea*
[3]*Department of Physics, Korea Advanced Institute of Science and Technology, 373-1 Guseong-dong, Yuseong-gu, Daejeon, 305-701, Korea*
[4]*Currently with the Optoelectronics Research Centre, University of Southampton, Southampton, SO17 1BJ, UK*
[*] *ikhwang@chonnam.ac.kr*

Abstract: We report the axial strain dependence of two types of all-fiber acousto-optic tunable filters based on flexural and torsional acoustic waves. Experimental observation of the resonant wavelength shift under applied axial strain could be explained by theoretical consideration of the combination of acoustic and optical effects. We discuss the possibility of suppressing the strain effect in the filters, or conversely, the possibility of using the strain dependence for wavelength tuning or strain sensors.

OCIS codes: (060.2310) Fiber optics; (230.1040) Acousto-optical devices.

References and links

1. H. S. Kim, S. H. Yun, I. K. Hwang, and B. Y. Kim, "All-fiber acousto-optic tunable notch filter with electronically controllable spectral profile," Opt. Lett. **22**, 1476-1478 (1997).
2. K. J. Lee, D. -I. Yeom, and B. Y. Kim, "Narrowband, polarization insensitive all-fiber acousto-optic tunable bandpass filter," Opt. Express **15**, 2987-2992 (2007), http://www.opticsinfobase.org/abstract.cfm?URI=oe-15-6-2987.
3. K. J. Lee, H. C. Park, and B. Y. Kim, "Highly efficient all-fiber tunable polarization filter using torsional acoustic wave," Opt. Express **15**, 12362-12367 (2007), http://www.opticsinfobase.org/abstract.cfm?URI=oe-15-19-12362.
4. Q. Li, A. A. Au, C.-H. Lin, I. V. Tomov, and H. P. Lee, "Performance characteristics of a WDM channel monitor based on an all-fiber AOTF with an on-fiber photodetector," IEEE Photon Technol. Lett. **15**, 718-720 (2003).
5. J. Zhao, X. Liu, Y. Wang, and Y. Luo, "Bending effect on fiber acousto-optic mode coupling," Appl. Opt. **44**, 5101-5104 (2005).
6. H. C. Park, B. Y. Kim, and H. S. Park, "Apodization of elliptical-core two-mode fiber acousto-optic filter based on acoustic polarization control," Opt. Lett. **30**, 3126-3128 (2005).
7. A. Diez, G. Kakarantzas, T. A. Birks, and P. St. J. Russell, "High strain-induced wavelength tunability in tapered fibre acousto-optic filters," Electron. Lett. **36**, 1187-1188 (2000).
8. H. Li, Y. Zhang, C. Wen, and Y. C. Soh, "Strain effect on the tunability of cascading all-fiber acoustic-optical tunable filters," Opt. Commun. **247**, 65-84 (2005).
9. H. Li, Y. Zhang, C. Wen, and Y. C. Soh, "Tunable stopband filter by using differential strains in all-fiber acoustooptical filter," J. Lightwave Technol. **17**, 609-611 (2005).
10. H. Li, Y. Zhang, C. Wen, and Y. C. Soh, "Design of tunable composite spectrums using all-fiber acoustooptical filters subject to strain control," J. Lightwave Technol. **24**, 1855-1864 (2006).
11. K. F. Graff, *Wave Motion in Elastic Solids* (Ohio State University Press, 1975), Chap. 3.
12. J. N. Blake, B. Y. Kim, and H. J. Shaw, "Fiber-optic modal coupler using periodic microbending," Opt. Lett. **11**, 177-179 (1986).
13. T. Yoshino, K. Kurosawa, K. Itoh, and T. Ose, "Fiber-optic Fabry-Perot interferometer and its sensor applications," IEEE J. Quantum Electron. **18**, 1624-1633 (1982).
14. J. N. Blake, S. Y. Huang, B. Y. Kim, and H. J. Shaw, "Strain effects on highly elliptical core two-mode fibers," Opt. Lett. **12**, 732-734 (1987).
15. D. Östling and H. E. Engan, "Narrow-band acousto-optic tunable filtering in a two-mode fiber," Opt. Lett. **20**, 1247-1249 (1995).
16. S. S. Lee, H. S. Kim, I. K. Hwang, and S. H. Yun, "Highly-efficient broadband acoustic transducer for all-fibre acousto-optic devices," Electron. Lett. **39**, 1309-1310 (2003).

#105687 - $15.00 USD Received 23 Dec 2008; revised 2 Feb 2009; accepted 2 Feb 2009; published 5 Feb 2009

17. K. J. Lee, K. S. Hong, H. C. Park, and B. Y. Kim, "Polarization coupling in a highly birefringent photonic crystal fiber by torsional acoustic wave," Opt. Express **16**, 4631-4638 (2008), http://www.opticsinfobase.org/abstract.cfm?URI=oe-16-7-4631.
18. M. Berwick, C.N. Pannell, P. St. J. Russell, and D. A. Jackson, "Demonstration of birefringent optical fibre frequency shifter employing torsional acoustic waves," Electron. Lett. **27**, 713-715 (1991).
19. S. Dey, "Torsional wave under initial stress," Pure Appl. Geophys. **94**, 53-59 (1972).
20. S. Dey and D. Dutta, "Torsional wave propagation in an initially stressed cylinder," Proc. Indian Natl. Sci. Acad. **58**, 425-429 (1992).
21. M. M. Selim, "Torsional waves propagation in an initially stressed dissipative cylinder," Appl. Math. Sci. **1**, 1419-1427 (2007).
22. S. Y. Huang, J. N. Blake, and B. Y. Kim, "Perturbation effects on mode propagation in highly elliptical core two-mode fibers," J. Lightwave Technol. **8**, 23-33 (1990).
23. Y. Ohtsuka, T. Ando, Y. Imai, and M. Imai, "Modal birefringence measurements of polarization-maintaining single-mode fibers without and with stretching by optical heterodyne interferometry," J. Lightwave Technol. **5**, 602-607 (1987).

1. Introduction

Tunable wavelength filters are key components for optical sensors and communication systems. In particular, all-fiber acousto-optic tunable filters (AOTFs) have attracted considerable interest because of their advantages such as wide and fast wavelength tuning and variable attenuation via simple electronic control [1-3]. Flexural and torsional acoustic waves were used in the all-fiber AOTFs. The flexural wave produces coupling between symmetric and anti-symmetric spatial modes, while the torsional wave produces coupling between the two orthogonal polarization modes. For practical applications of these devices, it is important to understand the effects of various external perturbations such as temperature fluctuation, fiber bending, twist, and axial strain on the device performances [4-7]. Among the perturbations, the axial strain is one of the most critical factors since the fiber strain is highly dependent on a packaging structures and usually temperature sensitive due to the thermal expansion of fibers and fiber holders. The fiber strain induces the changes in both optical and acoustic properties of the fiber, resulting in considerable changes in the filter wavelengths. There have been a few reports on the strain effect of AOTF, but they deal with only flexural-mode AOTF using tapered fibers where the optical effect is negligible in compared to the acoustic effect [7-10].

In this paper, we describe the axial strain dependence of two types of AOTFs based on flexural and torsional acoustic waves using a standard single-mode fiber (for flexural wave) or a high-birefringence fiber (for torsional wave). We found that both the optical and the acoustical properties of the fibers are significantly affected by the strain, and the strain-induced shifts in the coupling wavelength could be successfully explained by the combination of the two effects.

2. Axial strain dependence of the all-fiber AOTF using flexural acoustic wave

In the all-fiber AOTFs, the acousto-optic (AO) coupling between the two optical modes occurs at a resonant wavelength, which is determined by the following phase-matching condition: the acoustic wavelength (Λ) should be the same as the optical beatlength (L_B) between two modes,

$$\Lambda(\varepsilon) = L_B(\lambda, \varepsilon), \tag{1}$$

where, ε and λ denote the axial strain and the optical wavelength, respectively. When the axial strain is applied to the AO interaction region, both the acoustic wavelength and the optical beatlength change, resulting in the shift of the resonant wavelength, λ. Here the two changes are referred to acoustic and optical effect, respectively. The acoustic effect for the flexural acoustic wave is considered first. In a cylindrical optical fiber whose diameter is much smaller than acoustic wavelengths, the frequency of flexural acoustic wave under the axial strain can be expressed as the following [11]:

#105687 - $15.00 USD Received 23 Dec 2008; revised 2 Feb 2009; accepted 2 Feb 2009; published 5 Feb 2009

$$f = \frac{2\pi}{\Lambda^2}\left[\left(\frac{EI}{\rho A}\right)\left(1+\frac{\Lambda^2 T}{4\pi^2 EI}\right)\right]^{1/2}, \tag{2}$$

where, I, E, ρ, A, and T denote the area moment of inertia, Young's modulus, the fiber density, the cross-sectional area of the fiber, and the initial tension in the longitudinal direction of the fiber, respectively. Because the area moment of inertia and Young's modulus are also given by

$$I = \frac{\pi}{4}a^4, \tag{3}$$

$$E \equiv \frac{T/A}{\delta l/l} = \frac{T/A}{\varepsilon}, \tag{4}$$

respectively, the wavelength variation of the lowest order flexural acoustic mode by axial strain is expressed as,

$$\frac{\delta\Lambda}{\Lambda} = \left[\frac{\sqrt{E/\rho}}{2\pi a f}\left\{\varepsilon + \left(\varepsilon^2 + \frac{4\pi^2 a^2 f^2}{E/\rho}\right)^{1/2}\right\}\right]^{1/2} - 1, \tag{5}$$

where, ε and a denote the axial strain and the fiber radius, respectively. Figure 1 shows the acoustic wavelength variation ($\delta\Lambda/\Lambda$) as a function of the fiber radius for the 1%-axial strain at the acoustic frequencies of 2.0 MHz, 2.5 MHz, and 3.0 MHz, respectively. The graph shows that the strain-induced acoustic effect becomes larger for the small fiber radius.

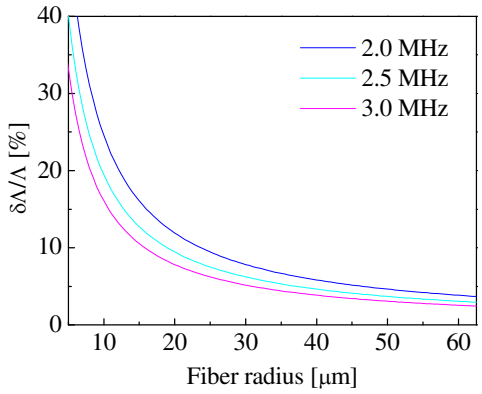

Fig. 1. Acoustic wavelength variation as a function of the fiber radius for the 1%-axial strain at the acoustic frequency of 2.0 MHz, 2.5 MHz, and 3.0 MHz, respectively.

Now the strain-induced optical effect is investigated. The optical beatlength between the first- and the second-order modes of a step-index fiber can be expressed as,

$$L_B = 2\pi a_{co}\left(\frac{2}{\Delta}\right)^{1/2} f(V), \tag{6}$$

where, a_{co}, Δ, V, and $f(V)$ denote the fiber core radius, the normalized core-cladding index difference, the normalized frequency, and the beatlength dispersion, respectively [12]. The change of optical beatlength is caused by changes of the core radius and the refractive indices under a strain. When a fiber of length l is stretched by a small amount δl, the beatlength change is given by,

#105687 - $15.00 USD Received 23 Dec 2008; revised 2 Feb 2009; accepted 2 Feb 2009; published 5 Feb 2009

$$\delta L_B = \frac{\partial L_B}{\partial l}\delta l = \left(\frac{\partial L_B}{\partial a}\frac{\partial a}{\partial l} + \frac{\partial L_B}{\partial \Delta}\frac{\partial \Delta}{\partial l} + \frac{\partial L_B}{\partial f}\frac{\partial f}{\partial V}\frac{\partial V}{\partial l} \right)\delta l \,, \tag{7}$$

and, using the relations in [13, 14], each term in Eq. (7) can be expressed as the following:

$$\frac{\partial L_B}{\partial a}\frac{\partial a}{\partial l} = -\sigma \frac{L_B}{l} \,, \tag{8}$$

$$\frac{\partial L_B}{\partial \Delta}\frac{\partial \Delta}{\partial l} = \frac{1}{2}\left[p_{12} - \sigma(p_{11} + p_{12}) \right] n^2 \frac{L_B}{l} \,, \tag{9}$$

$$\frac{\partial L_B}{\partial f}\frac{\partial f}{\partial V}\frac{\partial V}{\partial l} = -\left(\sigma + \left[p_{12} - \sigma(p_{11} + p_{12}) \right] n^2 \right) \frac{V}{f}\frac{\partial f}{\partial V}\frac{L_B}{l} \,, \tag{10}$$

respectively. Here, p_{11}, p_{12}, n, and σ are the strain-optic coefficients, the refractive index of fused silica, and Poisson's ratio, respectively. If we substitute Eqs. (8) - (10) into Eq. (7) and use the relationship $(V/f)(\partial f/\partial V) = -(\lambda/L_B)(\partial L_B/\partial \lambda)$ from Eq. (6), the variation of the optical beatlength by the axial strain is expressed as,

$$\frac{\delta L_B}{L_B} = \varepsilon \left(-\sigma + \frac{1}{2}\left[p_{12} - \sigma(p_{11} + p_{12}) \right] n^2 + \left(\sigma + \left[p_{12} - \sigma(p_{11} + p_{12}) \right] n^2 \right) \frac{\lambda}{L_B}\frac{\partial L_B}{\partial \lambda} \right). \tag{11}$$

Here, the values of p_{11}, p_{12}, and σ are 0.113, 0.252, and 0.16, respectively.

Figure 2(a) shows the acoustic and the optical effects as a function of the axial strain at the acoustic frequency of 1.89 MHz, which are the plots of Eq. (5) and (11) for the standard single mode fiber (SMF) of 125 μm in diameter. The acoustic effect is larger than the optical effect for the same magnitude of the strain, and their slopes are 3.9 and 1.2, respectively. The resonant wavelength shift of the AOTF under the simultaneous changes of the acoustic wavelength and the optical beatlength can be explained in Fig. 2(b) illustrating the optical beatlength as a function of the optical wavelength. Note that the resonant wavelength is found where the phase matching condition is satisfied, as marked by *A*. When an axial strain is applied, the optical beatlength L_B increases by amount of δL_B, and at the same time, the acoustic wavelength Λ shifts upward by amount of $\delta\Lambda$. Then the coupling wavelength is now found at *B*.

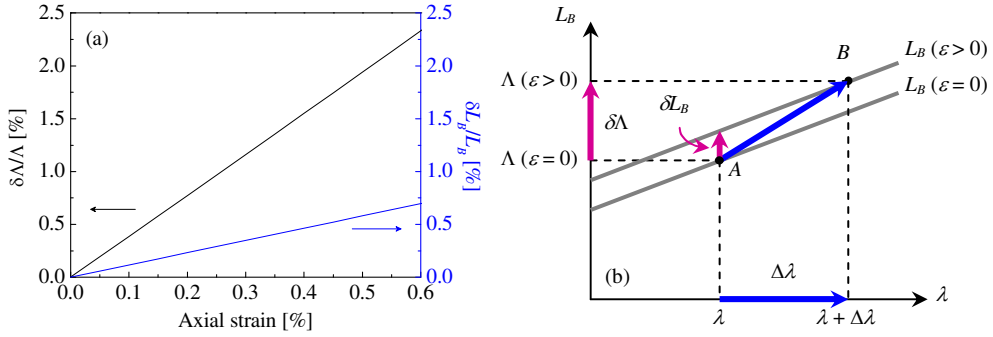

Fig. 2. (a) Variation of the acoustic wavelength and the optical beatlength as a function of the axial strain at the acoustic frequency of 1.89 MHz, and (b) the resonant wavelength shift of the AOTF using flexural acoustic wave by the strain.

This illustration shows the red-shift of the resonant wavelength under the positive strain. It should be noted that the acoustic effect works against the optical effect and reduces the strain effect. Therefore it could be possible to suppress the strain dependence in the flexural wave

#105687 - $15.00 USD Received 23 Dec 2008; revised 2 Feb 2009; accepted 2 Feb 2009; published 5 Feb 2009

AOTFs by proper design of optical or acoustic properties of the fiber. For example, a proper choice of outer diameter of the single mode fiber, so that $\delta\Lambda = \delta L_B$ holds, could be used for completely cancel the strain effect. It will be very useful for practical application of the device because it will remove some packaging issues related to the strain.

Figure 3 shows the schematic of the experimental setup for the measurement of the axial strain dependence of the all-fiber AOTF using flexural acoustic wave. The device is composed of an acoustic transducer, a standard SMF of 125 μm in diameter, and a fiber holding mount. The fiber is fixed at the two points using UV epoxy. On the right side, the fiber is bonded to a translation stage moving along the longitudinal axis of the fiber, so that the axial strain can be efficiently applied in the 18 cm-long AO interaction region between the two fixed points. The flexural acoustic wave generated by the coaxial acoustic transducer propagates along a bare section of the fiber and is absorbed by an acoustic damper (epoxy) at the end of the interaction region. The periodic micro-bends in the fiber induced by the flexural acoustic wave perturb the incident LP_{01} mode in the core and causes coupling to the anti-symmetric LP_{11} mode in the cladding at resonant wavelength where the phase matching condition is satisfied. The coupled LP_{11} mode is completely scattered or absorbed by the polymer jacket on the fiber before entering the optical spectrum analyzer, resulting in a wavelength notch in the transmission spectrum.

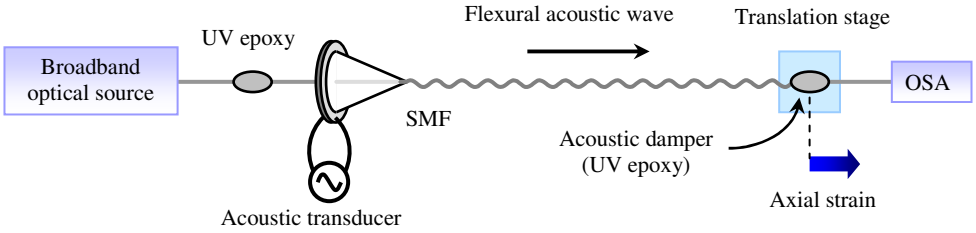

Fig. 3. Schematic for measurement of the axial strain dependence of the all-fiber AOTF using traveling flexural acoustic wave. OSA, optical spectrum analyzer.

Figure 4(a) shows the measured transmission spectra of the AOTF for various strains at the fixed acoustic frequency of 1.89 MHz, where the acoustic wavelength is 730 μm. The center wavelength of the filter shifts to the longer wavelength region with the increase of strain, as expected from Fig. 2 (b). The measured wavelength shift is plotted in Fig. 4(b) as a function of the axial strain, which agrees well with the theoretical calculations (red line) from Eq. (5) and (11). The graph shows the linear function with its slope of 22.0 nm/%. In case of the AOTF using tapered fibers reported in [7], the slope was about 410 nm/% at 2.555 MHz and it is much lager than our case with a standard single mode fiber. Its large slope can be explained by the large acoustic effect for a thin fiber as shown in Fig. 1. In contrast to the case of tapered fiber AOTF, the optical effect in the standard SMF AOTF is not negligible compared to the acoustic effect as discussed in Fig. 1 and 2(a). The blue line in the Fig. 2(b) shows the theoretical calculation when only the acoustic effect is considered [Eq. (5)], which confirms the importance of the optical effect. The 3-dB bandwidth of the all-fiber AOTF is proportional to the square of the optical beatlength (L_B) and the inverse of the AO interaction length (L_c) [15]. Both L_B and L_c increase with the increasing axial strain, and the strain effect on the 3-dB bandwidth is supressed. The notch depths of the AOTF were also insensitive to the variation of the axial strain because the acoustic energy, and therefore the coupling efficiency, in the fiber remains constant [16].

#105687 - $15.00 USD Received 23 Dec 2008; revised 2 Feb 2009; accepted 2 Feb 2009; published 5 Feb 2009

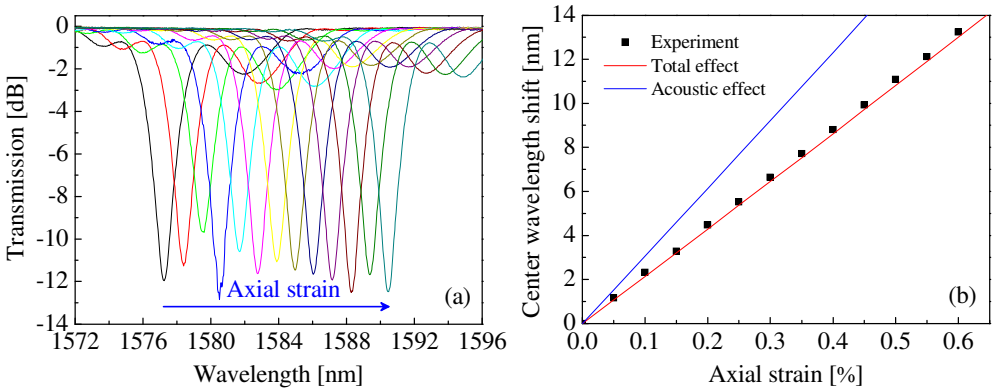

Fig. 4. (a) Measured transmission spectra of the all-fiber AOTF for the several applied the strain at the acoustic frequency of 1.89 MHz, and (b) the center wavelength shift of the AOTF as a function of the axial strain.

3. Axial strain dependence of the all-fiber AOTF using torsional acoustic wave

In all-fiber AOTF using torsional acoustic wave, the AO coupling occurs between the two linear polarization modes of a highly birefringent (HB) fiber [3, 17, 18]. As in the case of the AOTF using flexural acoustic wave, the strain induces both acoustic and optical effects in the fiber, and shifts the resonant wavelength of the device. In a cylindrical optical fiber, the equation of motion for torsional acoustic wave under the initial tension (T) can be expressed as,

$$G'\left(\frac{\partial^2 u_\theta}{\partial r^2}-\frac{u_\theta}{r^2}+\frac{1}{r}\frac{\partial u_\theta}{\partial r}\right)+\left(G'-\frac{T}{2}\right)\frac{\partial^2 u_\theta}{\partial z^2}=\rho'\frac{\partial^2 u_\theta}{\partial t^2}, \tag{12}$$

where, G and u_θ denote the shear modulus and the angular displacement in the cross-section of the fiber, respectively [19-21]. The primes in Eq. (12) mean the values modified by the strain. Using the definition of Poisson's ratio, $\partial a/\partial l = -\sigma(a/l)$, the density variation under the strain is given by,

$$\rho' = \rho + \delta\rho = \rho(1+\varepsilon-2\varepsilon\sigma). \tag{13}$$

From Eq. (12) and (13), the propagation velocity (v) of the lowest order torsional acoustic mode under the strain is given by,

$$\frac{\mathrm{v}'}{\mathrm{v}}=\frac{1+\varepsilon}{\sqrt{1-\varepsilon+2\sigma\varepsilon}}. \tag{14}$$

Because the acoustic velocity is simply given by the product of the acoustic frequency and the corresponding wavelength, the acoustic wavelength variation by the axial strain can be expressed as the following:

$$\frac{\delta\Lambda}{\Lambda}=\frac{1+\varepsilon}{\sqrt{1+\varepsilon-2\sigma\varepsilon}}-1. \tag{15}$$

Here, we assumed the homogeneous property for the fiber, and this estimation may contain some errors when the fiber has internal structures with strong stress field profile like HB fibers.

The strain-induced change of polarization beatlength of elliptical-core fiber has been reported in [22], where only the geometrical effect was considered. However, in case of the HB fibers having strong stress field distribution in the cross-section such as a HB fiber with

#105687 - $15.00 USD Received 23 Dec 2008; revised 2 Feb 2009; accepted 2 Feb 2009; published 5 Feb 2009

stress members or an e-core fiber with highly Ge-doped core, the stress field variation by the strain can seriously change the birefringence of the fiber [23]. In such fibers, the theoretical estimation of the polarization beatlength variation by the strain is very complicated since it requires detailed information about the stress field in the fiber cross-section. In addition, because the stress field profiles in the HB fibers and their strain-induced variation depend on each manufacturer, the strain-induced variation of the polarization beatlength also depends on the manufacturers. Therefore, we performed a simple experiment to measure the strain-induced change of polarization beatlength as following. Figure 5(a) shows the measurement setup. A broadband amplified spontaneous emission (ASE) from an Erbium doped fiber amplifier (EDFA) with the wavelength range of 1520 nm to 1620 nm was used as an incoherent and unpolarized light source. The cross-section of the HB fiber (3M^{TM}) with an elliptical stress member used in the experiment is shown in the inset of Fig. 5(c). The diameter of the HB fiber was 125 μm as in the case of the standard SMF. The two ends of the HB fiber are spliced with SMFs and the splice points were tightly fixed by UV epoxy on translation stages moving along the longitudinal axis of the fiber. The axial strain is applied in the same way as described in Fig. 3. The axes of the two polarizers are adjusted to get maximum visibility of the interference fringes in the transmission spectrum monitored at an optical spectrum analyzer (OSA), which corresponds to the polarizer angles of ±45 degrees with respect to the birefringent axes of the HB fiber.

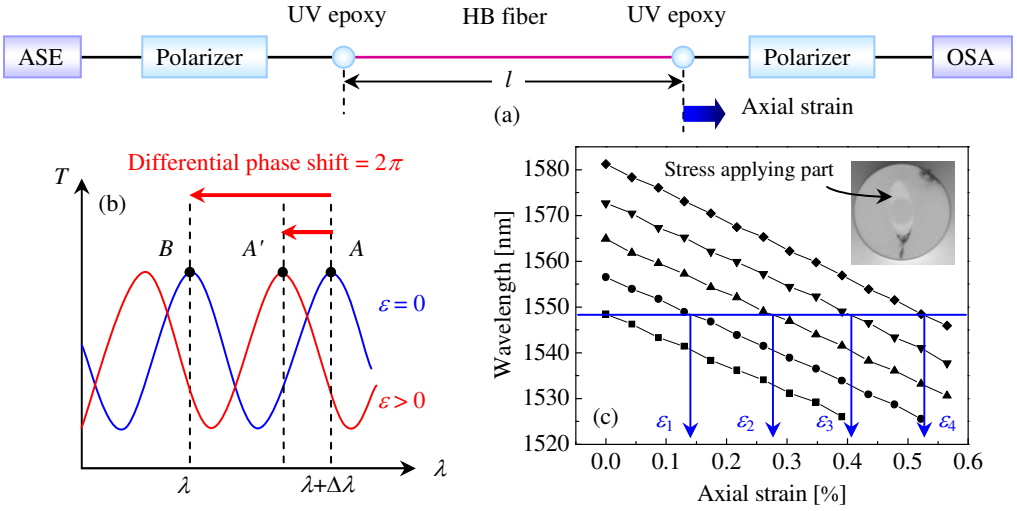

Fig. 5. (a) Setup for measurement of the variation of the polarization beatlength by the axial strain induced in the HB fiber, (b) the typical transmission spectrum at the OSA when the strain is being applied and not, and (c) the shift of the several modulation peaks by the strain induced in the measured HB fiber (stress-induced birefringence). Each value of ε_m means the axial strain required to shift the original peak to m-th peak in the direction of the short wavelength region. The inset shows the cross-section view of the HB fiber with elliptical stress member used in this experiment.

Figure 5(b) shows the typical transmission spectra with the periodic modulation as functions of wavelength. In the transmission curve without strain, the differential phase shift between the two eigen polarizations ($\Delta\beta(\lambda)\cdot l$) satisfy the following relationship.

$$\Delta\beta(\lambda+\Delta\lambda)\cdot l-\Delta\beta(\lambda)\cdot l=\frac{-2\pi}{L_B^2}\frac{\partial L_B}{\partial\lambda}\Delta\lambda\cdot l\,. \tag{16}$$

Here, $\Delta\beta$ denotes the birefringence between two polarization eigenmodes in the HB fiber and l is the length of the HB fiber. For the neighboring peaks in Fig. 5(b), the right side of the Eq.

#105687 - $15.00 USD Received 23 Dec 2008; revised 2 Feb 2009; accepted 2 Feb 2009; published 5 Feb 2009

(16) becomes $-2m\pi$, where $m > 0$ is an integer for positive values of $\partial L_B/\partial\lambda$ and $\Delta\lambda$, and therefore the following equation holds,

$$\Delta\beta(\lambda+\Delta\lambda)\cdot l + 2m\pi = \Delta\beta(\lambda)\cdot l\,. \tag{17}$$

For the adjacent peaks *A* and *B* in the Fig. 5(b), $m = 1$. When an axial strain is applied to the fiber, the whole transmission curve shifts to the short wavelength region and the point *A* also shifts to the point *A′*. When the differential phase shift changes by 2π due to the applied strain, the point *A′* reaches to the point *B*. For a general case of elongating the fiber by δl to move a peak by *m* peaks in the original spectrum, the change in the differential phase shift ($\Delta\beta(\lambda)\cdot l$) can be expressed as,

$$\delta(\Delta\beta)\cdot l + \Delta\beta\cdot\delta l = -\frac{2\pi}{(L_B)^2}\delta L_B\cdot l + \frac{2\pi}{L_B}\cdot\delta l = 2m\pi\,. \tag{18}$$

Now the strain-induced variation of the polarization beatlength is given from Eq. (18) as follows,

$$\frac{\delta L_B}{L_B} = \varepsilon_m - m\frac{L_B}{l}\,. \tag{19}$$

Here, ε_m denotes the axial strain required to shift the original peak to *m*-th peak in the direction of the short wavelength region. The shifts of the five transmission peaks by the strain and the several lowest ε_m values are shown in Fig. 5(c).

Figure 6(a) shows the variation of acoustic wavelength and the polarization beatlength as functions of the axial strain at the acoustic frequency of 1.332 MHz, which are the plots of Eq. (15) and (19). In order to plot the Eq. (19), we used the ε_m values measured in Fig. 5(c). Note that the calculation for the acoustic wave variation [Eq. (15)] did not include the effect of internal stress in the HB fiber, and therefore will not accurately predict the actual measurement for most of the commercially available HB fibers. The optical effect is larger than the acoustic effect, and their slopes are -3.7 and 0.7, respectively. Both effects push the resonant wavelength to a longer one, as shown in Fig. 6(b), resulting in large increase of resonant wavelength under a positive strain.

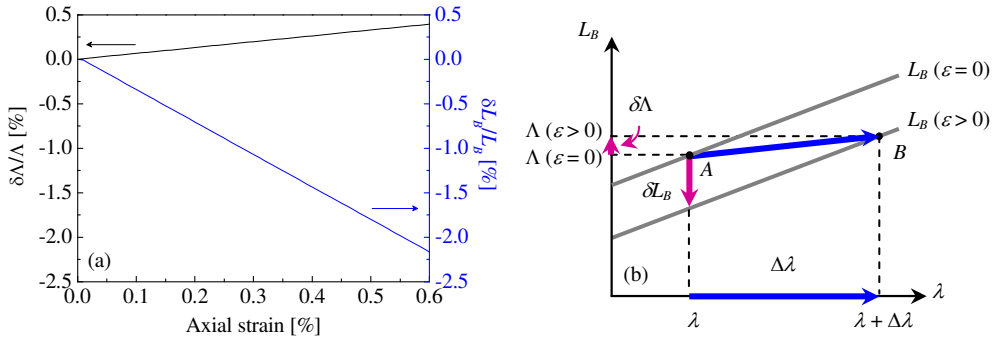

Fig. 6. (a) Variation of the acoustic wavelength and polarization beatlength as a function of the axial strain at the acoustic frequency of 1.332 MHz, and (b) the resonant wavelength shift of the AOTF using torsional acoustic wave by the strain.

Figure 7 shows the schematic of an experimental setup used for the measurement of the axial strain dependence of the all-fiber AOTF using torsional acoustic wave. The AO interaction length of the AOTF was 60 cm long. The configuration of the device is very similar to that of Fig. 3, but it has different lead zirconate titanate (PZT) acoustic transducer configuration for the generation of a torsional wave. It uses two pieces of PZT half-discs with opposite polling directions. When a radio frequency (RF) electric signal is applied, they

#105687 - $15.00 USD Received 23 Dec 2008; revised 2 Feb 2009; accepted 2 Feb 2009; published 5 Feb 2009

oscillate in opposite direction to effectively twist the horn. The torsional acoustic wave perturbs the input (horizontal) polarization of the LP_{01} mode and cause the energy transfer to orthogonal (vertical) polarization of the LP_{01} mode. Only the coupled light is selected by the output vertical polarizer.

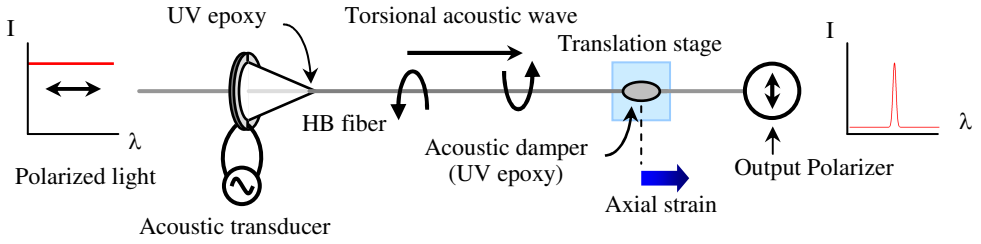

Fig. 7. Schmatic for measurement of the axial strain dependence of the all-fiber AOTF using traveling torsional acoustic wave.

Figure 8(a) shows the measured transmission spectra of the AOTF for the several different strains at the acoustic frequency of 1.332 MHz. The center wavelength of the filter shifts to the longer wavelength region with the increase of strain, as shown in Fig. 8(a). As in the case of the AOTF using the flexural acoustic wave, the 3-dB bandwidth and the coupling efficiency were not sensitive to the variation of the applied axial strain. The measured center wavelength shift of the AOTF is plotted in Fig 8(b) as a function of the axial strain, which shows a linear response to the strain. The slope of the measured center wavelength shift was 147.5 nm/%, which is much larger than the value of 58.4 nm/% estimated from Fig. 6. This discrepancy comes from the fact that we did not take into account in Eq. (15) the effect of strong internal stress in the HB fiber as discussed earlier. The acoustic dispersion can be changed by not only the strain applied in the longitudinal direction of the fiber [Eq. (14)] but also the stress field variation in the fiber cross-section. Nevertheless, because the slope and the linearity of the measured center wavelength shift by the strain are highly stable and reproducible, the controlled applied strain can be a new degree of freedom for wavelength tuning property of the all-fiber AO devices.

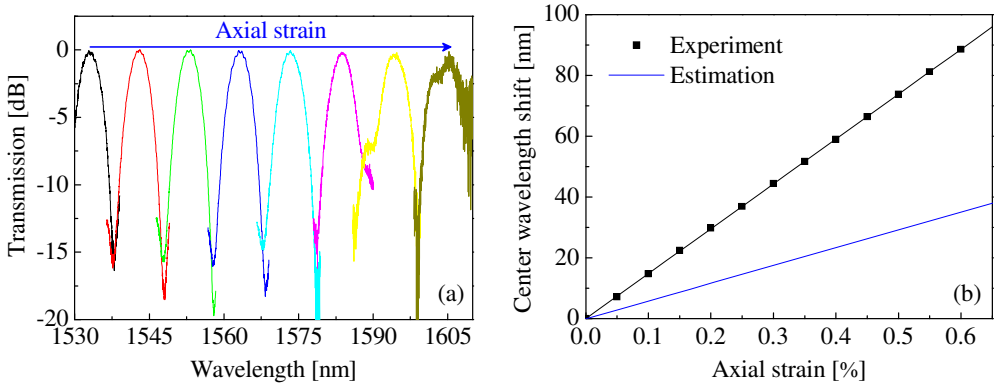

Fig. 8. (a) Measured transmission spectra of the all-fiber AOTF for the several applied the strain at the acoustic frequency of 1.332 MHz, and (b) the center wavelength shift of the AOTF as a function of the axial strain induced in the stress type HB fiber.

4. Conclusion

In conclusion, we have demonstrated and analyzed the axial strain dependence of two types of all-fiber acousto-optic tunable filters using flexural and torsional acoustic waves, respectively. The axial strain applied in AO interaction region changed both the acoustic and the optical properties of the optical fiber, resulting in center wavelength shift. In case of the flexural wave AOTF, the acoustic effect occurs to compensate the optical effect and reduce the resonance

#105687 - $15.00 USD Received 23 Dec 2008; revised 2 Feb 2009; accepted 2 Feb 2009; published 5 Feb 2009

shift, and therefore the strain dependence can be washed out by proper selection or design of the fiber. In case of the torsional wave AOTF, the acoustic and optical effects work together to increase the resonant shift.

The strain dependence can be positively utilized to tune the resonance wavelength, instead of changing acoustic frequencies. Wavelength tuning with a fixed acoustic frequency will be attractive since the acoustic transducer can be designed to have a sharp and strong resonance at the target frequency. We expect the maximum tuning ranges by the pure strain are about 14 nm and 100 nm for flexural wave and torsional wave AOTFs, respectively, which values are determined by the tensile strength of the fiber. The highly linear response of the resonant wavelength to the strain and good reproducibility promises a new degree of freedom for wavelength tuning in the all-fiber AO devices. The AOTF itself also can be used as a strain sensor. The strain sensor based on AOTF will be composed of a laser, an AOTF, and a detector, without the need of optical spectrum analyzer, and the wavelength shift can be monitored by sweeping the acoustic frequencies to locate the coupling resonance.

Acknowledgment

This work was supported by the Regional Research Center for Photonic Materials and Devices, Chonnam National University, and the Korea Research Foundation under Grant R08-2004-000-10503-0.

#105687 - $15.00 USD Received 23 Dec 2008; revised 2 Feb 2009; accepted 2 Feb 2009; published 5 Feb 2009